19

Dipartimento di Fisica
Universitá di Roma "La Sapienza"
I.N.F.N. - Sezione di Roma

ROME1-1115/95
October 23, 1995

Rome1-1115/95
Fermilab Library
0 1160 0049712 7

D.Fargion, R.V.Konoplich and A.Salis

COHERENT AND INCOHERENT INVERSE COMPTON SCATTERING ON LASER BEAM AND MONOCHROMATIC ISOTROPIC RADIATION

ROME prep. INFN n.1115

COHERENT AND INCOHERENT INVERSE COMPTON SCATTERING ON LASER BEAM AND MONOCHROMATIC ISOTROPIC RADIATION

Daniele Fargion,[1,2] Rostislav V. Konoplich[1,2] and Andrea Salis[1]

[1] *Dipartimento di Fisica, Universita' di Roma "La Sapienza", Rome*
P.le A. Moro 2, 00185 Rome, Italy.
[2] *INFN-Sezione di Roma I, c/ o Dipartimento di Fisica,*
Universita' di Roma "La Sapienza", 00185 Rome, Italy INFN, Rome

Abstract

Most of the known literature on incoherent Inverse Compton Scattering (ICS) is based on earliest theoretical attempts and later approximations led by F.C.Jones and J.B.Blumenthal. We found an independent and more general analytical procedure which provide both *relativistic* and *ultrarelativistic* limits for ICS while keeping care of the *coherent* and the *incoherent* nature of the process. These new analytical expressions can be derived in a straightforward way and they contain the previously reminded Jones' results. Our detailed solutions may be probed by already existing as well future ICS experiments. The coherent nature of the process may amplify the ICS process leading to a powerful ICS and offering a non perturbative diagnostic tool for the distribution of charges in the bunch. The Coherent Inverse Compton Scattering (CICS) could be better observed at relativistic regime when a laser beam hits on the back a travelling charge bunch.

e-mail:FARGION@ROMA1.INFN.IT
e-mail:KONOPLIC@ETP.MEPI.MSK.SU
e-mail:SALIS@ROMA1.INFN.IT
Tel:39 6 4991-4287 (Fargion)
fax:4957697

Preprint INFN n.1115 25 Settembre 1995

Introduction

The ICS plays a relevant role in a variety of recent high energy astrophysics (cosmic ray lifetime, gamma astronomy, gamma jets, ultrahigh energy cosmic rays (UHECR),...) as well as in high energy physics at LEP I, LEP II and linear accelerators . In particular the ICS of cosmic rays onto electromagnetic fields, either cosmological Black Body Radiation (BBR) at $T \approx 2.73\ K$ or diffused gray body as interstellar lights and radio waves or even nearly stationary magnetic fields, is source of high energy photons (X, gamma ,...) which we may observe as diffused or smeared pointlike gamma sources. The ICS onto BBR plays an important role in the complex connection between cosmic rays and gamma spectra and in the gamma burst puzzle. In this paper we derive the general ICS formulae for the interaction between a monochromatic electron beam and a monochromatic photon beam, as a laser, either unidirectional or isotropic. We shall show that our results generalize and slightly correct previous known ones [1-5]. The complexity of the ICS onto a Planckian spectrum has already been experimentally verified [6,7] as well as successfully theoretically predicted [8,9].

The ICS on a monochromatic and unidirectional photon beam

To find the ICS spectrum we consider first the photon beam distribution in the Laboratory Frame (LF) (not to be confused with the electron rest frame EF) where this beam distribution is unidirectional and monochromatic; then we transform it in the (EF) where it still is unidirectional and monochromatic; in that frame (EF) we consider the normal Compton or Thomson scattering and finally we transform back the resulting diffused differential photon number to the LF.

Let us consider such a monochromatic and unidirectional photon beam in the LF : the differential number density per unit energy ϵ_o and solid angle Ω_o can be written as:

$$\frac{dn_o}{d\epsilon_o d\Omega_o} = n_o \delta(\epsilon_o - \hat{\epsilon}_o)\delta(\cos\theta_o - \cos\hat{\theta}_o)\delta(\varphi_o - \hat{\varphi}_o) \tag{1}$$

where $\hat{\theta}_o$ is the incident angle between the electron beam and photon beam directions and $\hat{\epsilon}_o$ is the initial photon energy in the LF. Our sources have an idealized beam with no spread both in angle and in energy. We transform now this distribution to the EF by standard Lorentz relations choosing as z axis the direction coincident with the electron momentum and reminding that $dn_o/d\epsilon_o$ is a relativistic invariant [2]. In the following we label by a * the quantities

related to the electron frame EF, so we have

$$\cos\theta_o = \frac{\cos\theta_o^* + \beta}{1+\beta\cos\theta_o^*}\ ,\ \varphi_o = \varphi_o^*\ ,\ \epsilon_o = \gamma\epsilon_o^*(1+\beta\cos\theta_o^*) \quad . \tag{2}$$

where β is the adimensional electron velocity and γ is the corresponding Lorentz factor. Using δ function properties the number density distribution, in the EF, becomes

$$\frac{dn_o^*}{d\epsilon_o^* d\Omega_o^*} = n_o\gamma(1-\beta\cos\hat{\theta}_o)\cdot$$
$$\cdot\,\delta[\epsilon_o^* - \gamma\hat{\epsilon}_o(1-\beta\cos\hat{\theta}_o)]\delta[\cos\theta_o^* - \hat{C}_o]\delta(\varphi_o^* - \hat{\varphi}_o) \tag{3}$$

where $\hat{C}_o = \theta_o^* = (\cos\hat{\theta}_o - \beta)/(1-\beta\cos\hat{\theta}_o)$ is the function describing the boosted cosine angle θ_o^*. Now we have to scatter and diffuse the photons in the EF; the function describing the differential number of diffused photons can be obtained as follows:

$$\frac{dN_1^*}{dt_1^* d\epsilon_1^* d\Omega_1^* d\epsilon_o^* d\Omega_o^*} = \frac{dn_o^*}{d\epsilon_o^* d\Omega_o^*}\frac{d\sigma_C}{d\epsilon_1^* d\Omega_1^*}c \tag{4}$$

where $\frac{d\sigma_C}{d\epsilon_1^* d\Omega_1^*}$ is the Klein-Nishina differential cross section

$$\frac{d\sigma_C}{d\epsilon_1^* d\Omega_1^*} = \frac{r_o^2}{2}\Big(\frac{\epsilon_1^*}{\epsilon_o^*}\Big)^2\Big(\frac{\epsilon_1^*}{\epsilon_o^*} + \frac{\epsilon_o^*}{\epsilon_1^*} - \sin^2\theta_{sc}^*\Big)\delta\Big(\epsilon_1^* - \frac{\epsilon_o^*}{1+\epsilon_o^*(1-\cos\theta_{sc}^*)/mc^2}\Big) \quad .$$

For most of the real ICS processes in present laboratories energetics it is possible to approximate the Klein-Nishina cross section by the Thomson cross section, *i.e.* $\epsilon_o^* \ll mc^2$, so we can consider

$$\frac{d\sigma_T}{d\epsilon_1^* d\Omega_1^*} = \frac{r_o^2}{2}(1+\cos^2\theta_{sc}^*)\delta(\epsilon_1^* - \epsilon_o^*) \tag{5}$$

where c is the speed of light. The dependence of σ_T by the inverse square electron mass leads us to consider mainly electron bunches. However our results can be applied also to protons where we have just a suppression factor $(m_e/m_p)^2$. The scattering angle in the EF must be expressed as a function of the other angles involved, *i.e.* the incoming θ_o^*,φ_o^* and the outcoming θ_1^*,φ_1^* angles

$$\cos\theta_{sc}^* = \sin\theta_o^*\sin\theta_1^*(\cos\varphi_o^*\cos\varphi_1^* + \sin\varphi_o^*\sin\varphi_1^*) + \cos\theta_o^*\cos\theta_1^* \quad . \tag{6}$$

It is interesting to notice that the distribution number $\frac{dN_1}{dt_1^* d\epsilon_1^* d\Omega_1^*}$ cannot be associated to any effective number density because of its intrinsic inhomogeneous nature. Finally we obtain the differential photon number per unit energy and solid angle in the LF by the inverse Lorentz transformations and we write it in the following integral form:

$$\frac{dN_1}{dt_1 d\epsilon_1 d\Omega_1} = \int_{\Omega_o^*}\int_{\epsilon_o^*}\frac{dN_1^*}{dt_1^* d\epsilon_1^* d\Omega_1^* d\epsilon_o^* d\Omega_o^*}\frac{dt_1^*}{dt_1}\frac{d\epsilon_1^*}{d\epsilon_1}\frac{d\Omega_1^*}{d\Omega_1}d\Omega_o^* d\epsilon_o^* \quad . \tag{7}$$

By sostitution of previous eqs.(4,6) and since $\frac{dt_1^*}{dt_1}\frac{d\epsilon_1^*}{d\epsilon_1}\frac{d\Omega_1^*}{d\Omega_1} = \frac{1}{\gamma^2(1-\beta\cos\theta_1)}$ the integral can be cast into the form

$$\frac{dN_1}{dt_1 d\epsilon_1 d\Omega_1} = \frac{n_o r_o^2 c}{2\gamma}\frac{(1-\beta\cos\hat{\theta}_o)}{(1-\beta\cos\theta_1)}\int_{\epsilon_o^*}\int_{\Omega_o^*}(1+\cos^2\theta_{sc}^*)\delta(\epsilon_1^*-\epsilon_o^*)\cdot$$

$$\cdot\,\delta[\epsilon_o^*-\gamma\hat{\epsilon}_o(1-\beta\cos\hat{\theta}_o)]\delta(\cos\theta_o^*-\hat{C}_o)\delta(\varphi_o^*-\hat{\varphi}_o)d\epsilon_o^* d\Omega_o^* \quad . \tag{8}$$

We perform the integrals and the final form for the differential photon number per unit energy and solid angle in the Laboratory Frame becomes

$$\frac{dN_1}{dt_1 d\epsilon_1 d\Omega_1} = \frac{n_o r_o^2 c}{2\beta\gamma^2\epsilon_1}\frac{(1-\beta\cos\hat{\theta}_o)}{(1-\beta\cos\theta_1)}\Big(1+C_1^2\hat{C}_o^2+(1-C_1^2)(1-\hat{C}_o^2)(\cos\varphi_1\cos\hat{\varphi}_o+$$

$$+\sin\varphi_1\sin\hat{\varphi}_o)^2+2C_1\hat{C}_o(1-C_1^2)^{1/2}(1-\hat{C}_o^2)^{1/2}(\cos\varphi_1\cos\hat{\varphi}_o+\sin\varphi_1\sin\hat{\varphi}_o)\Big)\cdot$$

$$\cdot\,\delta\Big[\cos\theta_1-\frac{1}{\beta}\Big(1-\frac{\hat{\epsilon}_o}{\epsilon_1}(1-\beta\cos\hat{\theta}_o)\Big)\Big] \quad . \tag{9}$$

where $C_1 = \cos\theta_1^* = (\cos\theta_1-\beta)/(1-\beta\cos\theta_1)$. The final ICS spectrum can be obtained by integrating over Ω_1 the previous equation and the result is:

$$\frac{dN_1}{dt_1 d\epsilon_1} = \frac{\pi n_o r_o^2 c}{2\beta\gamma^2\hat{\epsilon}_o}\Big[3-\hat{C}_o^2+(3\hat{C}_o^2-1)\frac{1}{\beta^2}\Big(\frac{\epsilon_1}{\gamma^2\hat{\epsilon}_o(1-\beta\cos\hat{\theta}_o)}-1\Big)^2\Big]. \tag{10}$$

Let us notice that this energy distribution does not depend on the initial azimuthal angle $\hat{\varphi}_o$ due to the axial symmetry of the problem. The ϵ_1 dependence shows that the original monochromatic and unidirectional photon spectrum has been spread into a final parabolic function. We show below its behaviour for some arbitrary parameters (fig.1-5). The spectrum is bound in energy by relativistic kinematics arguments and its extreme ϵ_1 allowed values are $\epsilon_{1min} = \hat{\epsilon}_o(1-\beta\cos\hat{\theta}_o)/(1+\beta)$ and $\epsilon_{1max} = \hat{\epsilon}_o(1-\beta\cos\hat{\theta}_o)/(1-\beta)$. The θ_1 angle is simply varying into the range $[0,\pi]$ and, as usual, the most populate angular region of the high energy ICS beam is contained inside a thin cone whose aperture is of order $1/\gamma$. If we substitute in eq.(10) ϵ_{1min} and ϵ_{1max} we get an equal height for the parabolic spectrum extremes:

$$\frac{dN_1}{dt_1 d\epsilon_1}_{|\epsilon_{1(min,max)}} = \frac{\pi n_o r_o^2 c}{\beta\gamma^2\hat{\epsilon}_o}[1+\hat{C}_o^2] \quad . \tag{11}$$

The spectrum has a minimum for $\epsilon_1 = \gamma^2\hat{\epsilon}_o(1-\beta\cos\hat{\theta}_o)$ and in this point its value is:

$$\frac{dN_1}{dt_1 d\epsilon_1}_{|min} = \frac{\pi n_o r_o^2 c}{2\beta\gamma^2\hat{\epsilon}_o}[3-\hat{C}_o^2] \quad . \tag{12}$$

The above expressions are the rigorous analytical spectra for Thomson ICS onto a monochromatic and unidirectional photon beam. From eq.(9) we can

also get the angular distribution of scattered photons and the total rate number:

$$\frac{dN_1}{dt_1 d\Omega_1} = \frac{n_o r_o^2 c}{2\gamma^2}\frac{(1-\beta\cos\hat{\theta}_o)}{(1-\beta\cos\theta_1)^2}[1 + C_1^2\hat{C}_o^2 + (1-C_1^2)(1-\hat{C}_o^2)(\cos\varphi_1\cos\hat{\varphi}_o +$$

$$+ \sin\varphi_1\sin\hat{\varphi}_o)^2 + 2C_1\hat{C}_o(1-C_1^2)^{1/2}(1-\hat{C}_o^2)^{1/2}(\cos\varphi_1\cos\hat{\varphi}_o + \sin\varphi_1\sin\hat{\varphi}_o)] \tag{13}$$

and

$$\frac{dN_1}{dt_1} = \sigma_T n_o c(1-\beta\cos\hat{\theta}_o) \quad . \tag{14}$$

The spectrum in eq.(10) may be tested on known records of ICS. Our eq.(10) also contains the non relativistic limit where, for $\beta \to 0$, one must recover the correct initial Dirac delta function $\delta(\epsilon_1 - \hat{\epsilon}_o)$.

ICS on a monochromatic and unidirectional electron beam beyond the Thomson limit

Let us consider now the ICS in the framework of quantum electrodynamics in order to obtain the exact Compton result for the corresponding particle distribution in the case of a monochromatic and unidirectional photon beam. Considering two Feynman diagrams which contribute to this process the standard calculations give us the following expressions for the matrix element (in this section we use $\hbar = c = 1$):

$$\mid \bar{M} \mid^2 = 2^5\pi^2 r_o^2 m^2\left(\left[m^2\left(\frac{1}{\kappa_o p_o} - \frac{1}{\kappa_1 p_o}\right) + 1\right]^2 + \frac{\kappa_1 p_o}{\kappa_o p_o} + \frac{\kappa_o p_o}{\kappa_1 p_o} - 1\right) \tag{15}$$

where $\kappa_o p_o = \hat{\epsilon}_o m\gamma(1-\beta\cos\hat{\theta}_o)$, $\kappa_1 p_o = \epsilon_1 m\gamma(1-\beta\cos\theta_1)$. The corresponding cross section is given by

$$d\sigma = \frac{1}{2^6\pi^2}\frac{\mid \bar{M} \mid^2}{(p_o\kappa_o)}\delta^{(4)}(p_o + \kappa_o - p_1 - \kappa_1)\frac{d^3\kappa_1}{\epsilon_1}\frac{d^3p_1}{E_1} \quad . \tag{16}$$

In the case of colliding beams the number of collisions per second can be obtained from the following relation

$$d\dot{N}_1 = L d\sigma \tag{17}$$

where L is the luminosity which is defined by [10]

$$L = n_o n_1 V(1-\beta\cos\hat{\theta}_o) \tag{18}$$

V is the unit volume in the LF. In our case $n_1 V = 1$, the density n_o was defined in eq.(1). Now integrating eq.16 over the corresponding variables we

obtain the following exact expression for the angular distribution of scattered photons:

$$\frac{dN_1}{dt_1 d\Omega_1} = n_o \frac{r_o^2}{2} \frac{m^2 \epsilon_1^2}{(p_o \kappa_o)^2} (1 - \beta \cos \hat{\theta}_o) \cdot$$
$$\cdot \left(\left[m^2 \left(\frac{1}{\kappa_o p_o} - \frac{1}{\kappa_1 p_o} \right) + 1 \right]^2 + \frac{\kappa_1 p_o}{\kappa_o p_o} + \frac{\kappa_o p_o}{\kappa_1 p_o} - 1 \right) \tag{19}$$

where

$$\epsilon_1 = \frac{\hat{\epsilon}_o m \gamma (1 - \beta \cos \hat{\theta}_o)}{\gamma m (1 - \beta \cos \theta_1) + \hat{\epsilon}_o (1 - \cos \theta_{sc})}$$

and the scattering angle is defined as in eq.(6) but in the LF. The energy spectrum of ICS is given by

$$\frac{dN_1}{dt_1 d\epsilon_1} = n_o \pi r_o^2 \frac{m}{\hat{\epsilon}_o \gamma} \left(\frac{\gamma m^5}{\hat{\epsilon}_o^2 A^{3/2}} \left[\epsilon_1 (\hat{\epsilon}_o + m\gamma\beta \cos \hat{\theta}_o) + \right.\right.$$
$$\left. + \beta (\hat{\epsilon}_o \cos \hat{\theta}_o + m\gamma\beta)(m\gamma(1 - \beta \cos \hat{\theta}_o) - \epsilon_1) \right] + \frac{\kappa_o p_o}{\hat{\epsilon}_o A^{1/2}} \left[1 - \frac{2m^2}{\kappa_o p_o} - 2 \left(\frac{m^2}{\kappa_o p_o} \right)^2 \right] +$$
$$+ \frac{1}{B^{1/2}} \left[\left(\frac{m^2}{\kappa_o p_o} \right)^2 + \frac{2m^2}{\kappa_o p_o} + \frac{\epsilon_1 \gamma m}{\kappa_o p_o} \right] + \frac{m\gamma\beta}{(\kappa_o p_o) B^{3/2}} (\hat{\epsilon}_o \cos \hat{\theta}_o + m\gamma\beta) \cdot$$
$$\left. \cdot (\kappa_o p_o - \epsilon_1 \gamma m - \epsilon_1 \hat{\epsilon}_o) \right) \tag{20}$$

where

$$A = m^2 \left(\gamma^2 \left[m\gamma\beta(1 - \beta \cos \hat{\theta}_o) + \epsilon_1 (\cos \hat{\theta}_o - \beta) \right]^2 + \epsilon_1^2 (1 - \cos^2 \hat{\theta}_o) \right)$$

$$B = \hat{\epsilon}_o^2 + m^2 \gamma^2 \beta^2 + 2 \hat{\epsilon}_o m \gamma \beta \cos \hat{\theta}_o$$

and

$$\frac{\hat{\epsilon}_o m \gamma (1 - \beta \cos \hat{\theta}_o)}{m\gamma + \hat{\epsilon}_o + \sqrt{B}} \leq \epsilon_1 \leq \frac{\hat{\epsilon}_o m \gamma (1 - \beta \cos \hat{\theta}_o)}{m\gamma + \hat{\epsilon}_o - \sqrt{B}}$$

These exact expressions reproduce and confirm all the results of previous section as Thomson limit cases. Therefore eq.(10) can be used for further calculations of ICS on an isotropic monoenergetic background within the Thomson limit. Expression (20) may find application when considering the most energetic accelerators where the colliding electron and photon beams are of high energy.

Coherent and Incoherent ICS

The coherent scattering of photons onto electrons plays a relevant role in enhancing the ICS response efficiency (which cannot anyway exceed the unitarity limit). The phenomenon may be quantitatively explained [10] keeping care of the phase shift effects due to both the Coulomb as well as the radiation

field terms of nearby charges. This effect is related to the behaviour of a bunch of charges to scatter coherently an incident photon when its wavelenght is comparable with the intercharge distance or, at best, when the electromagnetic waves encompass the whole bunch size. The coherent process needs a very peculiar physical set up to take place; indeed it is often difficult to reveal the relativistic CICS because the primordial photon energy $\hat{\epsilon}_o$, when seen in the EF, is for most $\hat{\theta}_o$ angles blueshifted: $\epsilon_o^* = \gamma\epsilon_o(1-\beta\cos\hat{\theta}_o)$. Therefore in such situation the photon wavelenght becomes shorter than the original one and it can only reduce the coherence and the ICS signal. Consider for instance a microwave-radio signal $\hat{\lambda}_o$ at cm wavelenght (just near the diffraction limits of the geometrical sizes of the beam pipe) incoming with $\hat{\theta}_o = \pi/2$ in the LF; this wave, in the EF, will be experienced at a shifted wavelenght $\lambda_o^* \approx \hat{\lambda}_o/\gamma \approx 10\ \mu m(\gamma/10^3)^{-1}(\hat{\lambda}_o/cm)$ where we choose as unity a Lorentz factor of 10^3 characteristic of present synchrotron accelerators. This wavelenght, for a characteristic bunch size of mm-cm, can lead only to a partial CICS and in addition the interaction lenght is small. We have the worst case when the electron beam suffers a head-on ICS ($\hat{\theta}_o = \pi$): the photon wavelenght becomes twice blueshifted in the EF and the efficiency is twice less than in the previous example.

The back illumination to enhance CICS

Therefore it is natural consider the back illumination ($\hat{\theta}_o = 0$) where the photon wavelenght is seen redshifted in the EF: $\lambda_o^* \approx 2\gamma\hat{\lambda}_o = 2\,mm\left(\frac{\gamma}{10^3}\right)\left(\frac{\hat{\lambda}_o}{1\mu m}\right)$, a lenght comparable with the characteristic bunch size. So let us consider a bunch where the charges, whose total number is N_b, are spread into an ideal cylindrical shape of lenght l_b and radius r_b. We remind that in the <u>*incoherent*</u> ICS the addition of sources simply implies that the total spectrum is

$$\frac{dN_{1\ tot}}{dt_1 d\epsilon_1} = N_b \frac{dN_1}{dt_1 d\epsilon_1} \quad .$$

When we are dealing with the <u>*coherent*</u> ICS in our ideal cylindrical beam shape and as long as $l_b/N_b < 2\gamma\hat{\lambda}_o < l_b$ we get a spectrum of the form

$$\frac{dN_{coh}}{dt_1 d\epsilon_1} = \left(\frac{\hat{\lambda}_o^*}{l_b}N_b\right)\frac{dN_{1\ tot}}{dt_1 d\epsilon_1} = \frac{\hat{\lambda}_o}{\gamma(1-\beta\cos\hat{\theta}_o)}\frac{N_b}{l_b}\left(N_b\frac{dN_1}{dt_1 d\epsilon_1}\right) \tag{21}$$

and for $\hat{\theta}_o = 0$

$$\frac{dN_{coh}}{dt_1 d\epsilon_1}(\hat{\theta}_o = 0) \approx \frac{2\ mm}{l_b}\left(\frac{\hat{\lambda}_o}{\mu m}\right)\left(\frac{\gamma}{10^3}\right)N_b^2\frac{dN_1}{dt_1 d\epsilon_1} \quad . \tag{22}$$

Let us show the behaviour of the previous result with respect to the variables involved:

1) the charge number in the bunch N_b: its growth leads to a quadratic growth in the CICS spectrum (as long as $l_b/N_b < 2\gamma\hat{\lambda}_o$)

2) the initial photon wavelenght $\hat{\lambda}_o$: its growth leads to a corresponding nearly quadratically growth in the CICS spectrum contrary to the incoherent case where the spectrum has a roughly linear dependence on $\hat{\lambda}_o$)

3) the bunch lenght l_b: the CICS spectrum grows as l_b^{-1} when we keep fixed all the other parameters (as long as $2\gamma\hat{\lambda}_o < l_b < 2\gamma\hat{\lambda}_o N_b$, otherwise CICS becomes l_b independent)

4) the incident angle $\hat{\theta}_o$: its importance is very sensitive because we must also consider the geometrical effect related to the laser beam and bunch size; in fact the interaction region L_o, where the two beams overlap, is roughly given by $L_o \sim r_b/\sin\hat{\theta}_o$ and so the total number of diffused photon grows as

$$N_1 \sim \frac{dN_1}{dt_1}\frac{L_o}{c} \sim \sigma_T n_o \frac{\hat{\lambda}_o r_b N_b^2}{\gamma l_b \sin\hat{\theta}_o} \quad . \tag{23}$$

For $\hat{\theta}_o \to 0$ we have $L_o \to L_{TOT}$ where L_{TOT} is the total allowable experimental lenght; for example the whole beam pipe lenght. This condition clearly shows that the best CICS photon production occurs when $\hat{\theta}_o = 0$

5) the Lorentz factor γ: its growth leads to a complicated behaviour of the spectrum but in the coherent regime $l_b/N_b < 2\gamma\hat{\lambda}_o < l_b$ the spectrum decreases as γ^{-1} while for $\gamma \gg l_b/\hat{\lambda}_o$ the coherent effect is saturated and the spectrum decreases as γ^{-2} (fig.6). This fact provides a very simple key signature of CICS effects. Moreover, as the ϵ_o^* photon energy is extremely low in the EF, the waves don't perturbate the bunch itself and so they can act as an ideal diagnostic tool to inspect the bunch structure.

The ICS onto a monochromatic and isotropic photon spectrum

In ref.[2] F.C. Jones found the ultrarelativistic ICS spectrum resulting from the interaction between high energy electrons and an isotropic and monochromatic photon spectrum. We show that his result can be obtained and slightly corrected by integrating eq.(10) over all permitted $\hat{\theta}_o$ angles. Our analytical and exact result can be set in a very compact form and it is derived from the following integral

$$\frac{dN_{1is}}{dt_1 d\epsilon_1} = \frac{1}{4\pi}\int_{\Omega_o} \frac{dN_1}{dt_1 d\epsilon_1} d\Omega_o =$$

$$= \frac{\pi n_o r_o^2 c}{4\beta\gamma^2\hat{\epsilon}_o}\int_{\hat{\theta}_{min}}^{\hat{\theta}_{max}} \left[3-\hat{C}_o^2+(3\hat{C}_o^2-1)\frac{1}{\beta^2}\left(\frac{\epsilon_1}{\gamma^2\hat{\epsilon}_o(1-\beta\cos\hat{\theta}_o)}-1\right)^2\right]\sin\hat{\theta}_o d\hat{\theta}_o \tag{24}$$

The upper and lower limits of this integral can be found from the inequality $\epsilon_{1min} \leq \epsilon_1 \leq \epsilon_{1max}$ where the minimum and maximum energies of scattered

photons were defined in the first section. Thus we obtain

$$\frac{1-\beta}{1+\beta}\hat{\epsilon}_o \le \epsilon_1 \le \hat{\epsilon}_o \qquad \frac{1}{\beta}\Big[1-\frac{\epsilon_1}{\hat{\epsilon}_o}(1+\beta)\Big] \le \cos\hat{\theta}_o \le 1$$

$$\hat{\epsilon}_o \le \epsilon_1 \le \frac{1+\beta}{1-\beta}\hat{\epsilon}_o \qquad -1 \le \cos\hat{\theta}_o \le \frac{1}{\beta}\Big[1-\frac{\epsilon_1}{\hat{\epsilon}_o}(1-\beta)\Big] \ .$$

As one can see from these expressions only photons incoming within a thin cone in the direction of the electron beam contribute to the lowest energy final photons meanwhile photons moving in the opposite direction contribute to the highest energy part of the spectrum. An elementary calculation gives

$$\frac{dN_{1is}}{dt_1 d\epsilon_1} = \frac{\pi n_o r_o^2 c}{4\beta^4\gamma^2\hat{\epsilon}_o}\Bigg(\Big[3\beta^2-2+\frac{3}{\beta^2}\Big]x + \frac{2}{\gamma^2}\Big[\Big(1-\frac{3}{\beta^2}\Big)\Big(1+\frac{\epsilon_1}{\hat{\epsilon}_o}\Big)\Big]\ln x +$$
$$+\frac{1}{\gamma^4}\Big[\Big(1-\frac{3}{\beta^2}\Big)\Big(1+\frac{\epsilon_1^2}{\hat{\epsilon}_o^2}\Big)-\frac{12\epsilon_1}{\beta^2\hat{\epsilon}_o}\Big]\frac{1}{x}+$$
$$+\frac{3\epsilon_1}{\beta^2\gamma^6\hat{\epsilon}_o}\Big(1+\frac{\epsilon_1}{\hat{\epsilon}_o}\Big)\frac{1}{x^2}-\frac{\epsilon_1^2}{\beta^2\gamma^8\hat{\epsilon}_o^2}\frac{1}{x^3}\Bigg)_{x_{min}}^{x_{max}} \tag{25}$$

where $x = (1-\beta\cos\hat{\theta}_o)$. We have now two different regions depending on the value assumed by the ratio $\epsilon_1/\hat{\epsilon}_o$: if $\frac{(1-\beta)\hat{\epsilon}_o}{1+\beta} \le \epsilon_1 \le \hat{\epsilon}_o$ then $x_{max} = [\epsilon_1(1+\beta)/\hat{\epsilon}_o]$ and $x_{min} = (1-\beta)$; if $\hat{\epsilon}_o \le \epsilon_1 \le \frac{(1+\beta)\hat{\epsilon}_o}{1-\beta}$ then $x_{max} = (1+\beta)$, $x_{min} = [\epsilon_1(1-\beta)/\hat{\epsilon}_o]$. The two separate formulae, left and right, must vanish respectively at $\epsilon_1 = \hat{\epsilon}_o(1-\beta)/(1+\beta)$ and $\epsilon_1 = \hat{\epsilon}_o(1+\beta)/(1-\beta)$ and they must obviously coincide for $\epsilon_1 = \hat{\epsilon}_o$. Labelling by L the left hand side and by R the right hand side, with respect to the value $\epsilon_1 = \hat{\epsilon}_o$, the two formulae, exact in the whole range of allowable values for the ratio $\epsilon_1/\hat{\epsilon}_o$, become

$$\frac{dN_{1is\ L}}{dt_1 d\epsilon_1} = \frac{\pi n_o r_o^2 c}{4\beta^6\gamma^2\hat{\epsilon}_o}\Bigg(\frac{\epsilon_1}{\hat{\epsilon}_o}(1+\beta)\Big[\beta(\beta^2+3)+\frac{1}{\gamma^2}(9-4\beta^2)\Big]+$$
$$+(1-\beta)\Big[\beta(\beta^2+3)-\frac{1}{\gamma^2}(9-4\beta^2)\Big]+$$
$$-\frac{2}{\gamma^2}(3-\beta^2)\Big(1+\frac{\epsilon_1}{\hat{\epsilon}_o}\Big)\ln\Big[\frac{\epsilon_1(1+\beta)}{\hat{\epsilon}_o(1-\beta)}\Big]-\frac{\hat{\epsilon}_o}{\gamma^4\epsilon_1}+\frac{\epsilon_1^2}{\gamma^4\hat{\epsilon}_o^2}\Bigg) \tag{26a}$$

and

$$\frac{dN_{1is\ R}}{dt_1 d\epsilon_1} = \frac{\pi n_o r_o^2 c}{4\beta^6\gamma^2\hat{\epsilon}_o}\Bigg((1+\beta)\Big[\beta(\beta^2+3)+\frac{1}{\gamma^2}(9-4\beta^2)\Big]+$$
$$+\frac{\epsilon_1}{\hat{\epsilon}_o}(1-\beta)\Big[\beta(\beta^2+3)-\frac{1}{\gamma^2}(9-4\beta^2)\Big]+$$
$$-\frac{2}{\gamma^2}(3-\beta^2)\Big(1+\frac{\epsilon_1}{\hat{\epsilon}_o}\Big)\ln\Big[\frac{\hat{\epsilon}_o(1+\beta)}{\epsilon_1(1-\beta)}\Big]+\frac{\hat{\epsilon}_o}{\gamma^4\epsilon_1}-\frac{\epsilon_1^2}{\gamma^4\hat{\epsilon}_o^2}\Bigg) \ . \tag{26b}$$

We notice that the two expressions exhibit some kind of symmetry, in particular the second one can be obtained from the first one simply by reversing

the β sign and multiplying the whole formula by (-1). The non relativistic limit $\beta \to 0$ in eq.(26a,b) leads to a monochromatic spectrum, *i.e.* a Dirac δ function, as it should be expected. Now we consider the ultrarelativistic limit $\beta \to 1$ and, neglecting terms smaller than $1/\gamma^2$ we get

$$\frac{dN_{1is\ L}}{dt_1 d\epsilon_1} \approx \frac{\pi n_o r_o^2 c}{2\gamma^4 \hat{\epsilon}_o \beta^6}\left[\left(4\gamma^2+2\right)\frac{\epsilon_1}{\hat{\epsilon}_o}+1-\frac{3}{2\gamma^2}-2\left(1+\frac{\epsilon_1}{\hat{\epsilon}_o}\right)\ln\left(\frac{4\gamma^2\epsilon_1}{\hat{\epsilon}_o}\right)-\frac{\hat{\epsilon}_o}{2\gamma^2\epsilon_1}\right] \quad (27a)$$

for $\frac{1}{4\gamma^2} < \frac{\epsilon_1}{\epsilon_o} \leq 1$ and

$$\frac{dN_{1is\ R}}{dt_1 d\epsilon_1} \approx \frac{\pi n_o r_o^2 c}{2\gamma^4 \hat{\epsilon}_o \beta^6}\left[4\gamma^2+2+\left(1-\frac{3}{2\gamma^2}\right)\frac{\epsilon_1}{\hat{\epsilon}_o}-2\left(1+\frac{\epsilon_1}{\hat{\epsilon}_o}\right)\ln\left(\frac{4\gamma^2\hat{\epsilon}_o}{\epsilon_1}\right)-\frac{\epsilon_1^2}{2\gamma^2\hat{\epsilon}_o^2}\right]. \quad (27b)$$

for $1 \leq \frac{\epsilon_1}{\epsilon_o} < 4\gamma^2$. These equations must be compared with eq.(40) and eq.(44) of ref.[2]. We note that we have a slight difference in a couple of terms and in the coefficient in front of the logaritmic term. From inspection of fig.7-8 one sees that Jones' approximated formulae exhibit a slight departure from our exact expressions and the difference is of order $1/\gamma^2$. Moreover it is also possible to notice that our eq.27 reppresent a better approximation for most of the $\epsilon_1/\hat{\epsilon}_o$ allowed values. At ultrarelativistic regime all the three kinds of expressions (eq.26, eq.27, Jones' approximations) are overlapping. For most applications where both non relativistic and ultrarelativistic regimes are of interest we consider our exact formula (26) which is more convenient to handle than the Jones' significantly more complicated expression eq.(35) in ref.[2].

Conclusions

We derived exact analytical formulae able to describe the ICS onto monochromatic beam lasers either in relativistic and non relativistic limits. Our results correct and extend previous known ones. These new formulae are to prefer because of their straightforward derivation and their more transparent form. We also discuss the coherence of ICS (CICS) pointing out how it could be reinforced and experimentally revealed. We underline different physical conditions for testing CICS and we consider in details the spectral dependence on the various free parameters. We probed that CICS has its maximal and optimal experimental set up when relativistic bunch of charges are hit by collinear back photon lasers (Back Laser Illumination BLI) at infrared wavelenghts. The BLI in CICS may offer a powerful diagnostic tool to study the bunch internal structure with negligible disturbance of the bunch structure itself. We will show elsewhere that our results on ICS onto BBR can successfully fit the known experimental data taken at LEP I in recent years. This process, ICS onto BBR, plays an important role also in astrophysical problems where the cosmic rays energy loss by ICS and its consequent ICS radiation in gamma rays is of primary relevance. ICS onto stellar BBR may also be important in

solving the well known GRB puzzle.

Acknowledgements

We wish to thank Dott. L.Silvestrini for useful comments.

References

[1] V.L.Ginzburg, S.I.Syrovatskii, Soviet Phys.JETP 19 (1964) 1255. SPHJA
[2] F.C.Jones, Phys.Rev. 167 (1968) 1159. PhRvA
[3] G.R.Blumenthal, R.J.Gould, Rev.Mod.Phys. 42 (1970) 237. RMPhA
[4] M.S.Longair, High Energy Astrophysics (Cambridge University Press, 1981).
[5] V.S.Berezinskii, S.V.Bulanov, V.A.Dogiel, V.L.Ginzburg, V.S. Ptuskin, Astrophysics of Cosmic Rays (North Holland, 1990).
[6] B.Dehning, A.C.Melissinos, P.Ferrone, C.Rizzo, G.von Holtey, Phys.Lett.B 249 (1990) 145. PhLtA
[7] C.Bini, G.De Zorzi, G.Diambrini-Palazzi, G.Di Cosimo, A.Di Domenico, P.Gauzzi, D.Zanello, Phys.Lett.B 262 (1991) 135. PhLtA
[8] A.Di Domenico, Particle Accelerators 39 (1992) 137. PlacB
[9] D.Fargion, A.Salis, Nucl.Phys.B (Proc.Suppl.) 43 (1995) 269.
[10] E.Segre', Nuclei e Particelle (Zanichelli, 1994) p.137.
[11] R.Coisson, Eur.J.Phys. 15 (1994) 29. EJPHD

Figure Captions

- **Fig.1**: The incoherent energy spectrum (eq.10) for $\hat{\theta}_o = 0$ (dash), $\hat{\theta}_o = \pi/2$ (dot), $\hat{\theta}_o = \pi$ (continuous)
- **Fig.2**: The incoherent energy spectrum (eq.10) for $\hat{\theta}_o = 0$ and $\gamma = 10$ (dash), $\gamma = 100$ (dot), $\gamma = 1000$ (continuous)
- **Fig.3**: The incoherent energy spectrum (eq.10) for $\hat{\theta}_o = \pi/2$ and $\gamma = 10$ (dash), $\gamma = 100$ (dot), $\gamma = 1000$ (continuous)
- **Fig.4**: The incoherent energy spectrum (eq.10) for $\hat{\theta}_o = \pi$ and $\gamma = 10$ (dash), $\gamma = 100$ (dot), $\gamma = 1000$ (continuous)
- **Fig.5**: The incoherent energy spectrum (eq.10) for $\hat{\theta}_o = \pi/2$, $\gamma = 100$ and $\hat{\epsilon}_o = 1\ eV$ (dash), $\hat{\epsilon}_o = 0.1\ eV$ (dot), $\hat{\epsilon}_o = 0.01\ eV$ (continuous)
- **Fig.6**: The coherent spectrum (eq.22) for $N_b = 2 \cdot 10^3$, $l_b = 2\ mm$, $\hat{\lambda}_o = 1\ \mu m$ and $\gamma = 10$ (continuous), $\gamma = 100$ (dash), $\gamma = 1000$ (dot), $\gamma = 10000$ (dot dash)
- **Fig.7**: The exact spectrum (eq.26) (continuous) and the approximations: Jones' (eq.40-44) (dash), eq.(27) (dot) for $\gamma = 2$
- **Fig.8**: The exact spectrum (eq.26) (continuous) and the approximations: Jones' (eq.40-44) (dash), eq.(27) (dot) for $\gamma = 5$

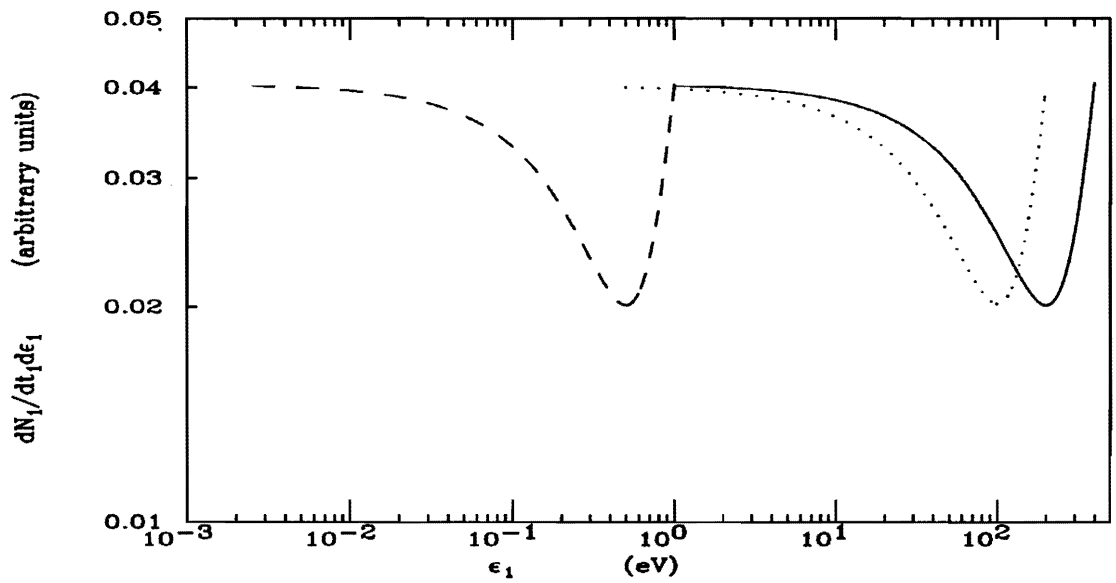
0.05
0.04
0.03
0.02
0.01
$dN_1/dt_1d\epsilon_1$ (arbitrary units)
10^{-3}
10^{-2}
10^{-1}
10^{0}
10^{1}
10^{2}
ϵ_1 (eV)

Figure 1:

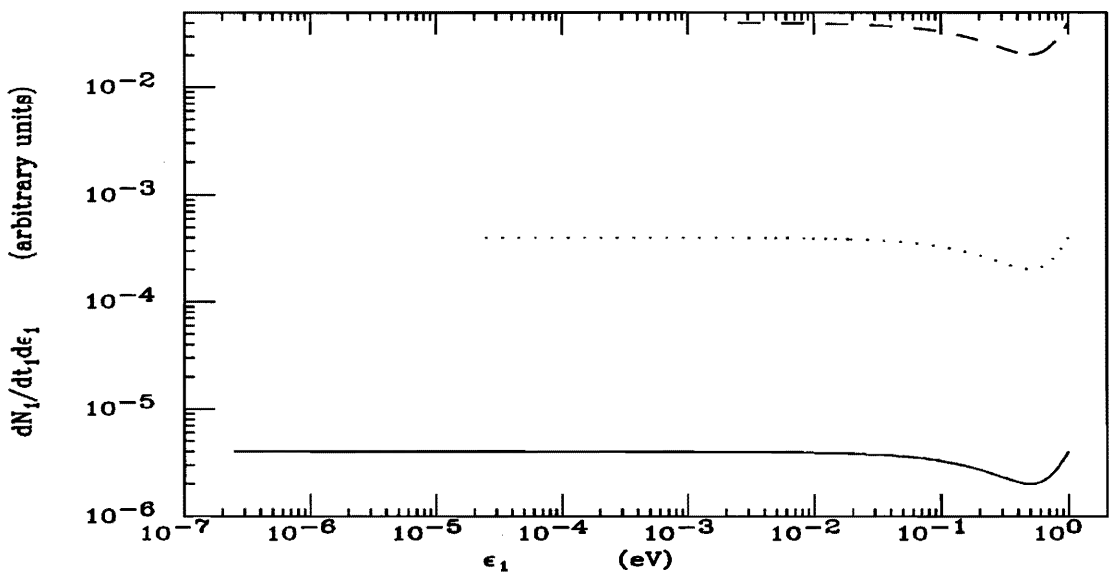
$dN_1/dt_1d\epsilon_1$ (arbitrary units)
10^{-2}
10^{-3}
10^{-4}
10^{-5}
10^{-6}
10^{-7}
10^{-6}
10^{-5}
10^{-4}
10^{-3}
10^{-2}
10^{-1}
10^{0}
ϵ_1 (eV)

Figure 2:

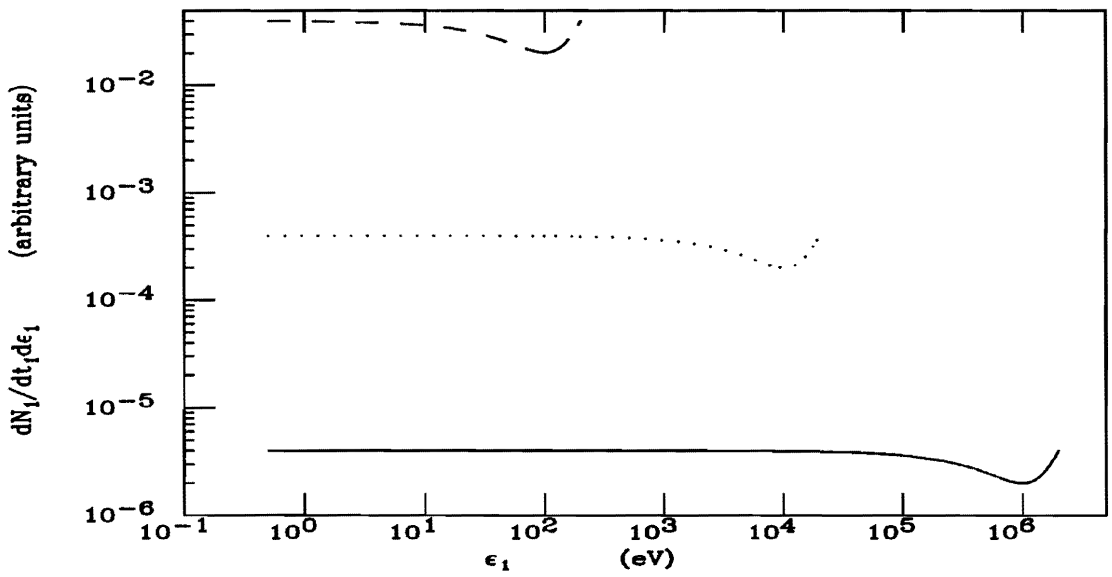
$dN_1/dt_1d\epsilon_1$ (arbitrary units)
10^{-2}
10^{-3}
10^{-4}
10^{-5}
10^{-6}
10^{-1}
10^{0}
10^{1}
10^{2}
10^{3}
10^{4}
10^{5}
10^{6}
ϵ_1
(eV)

Figure 3:

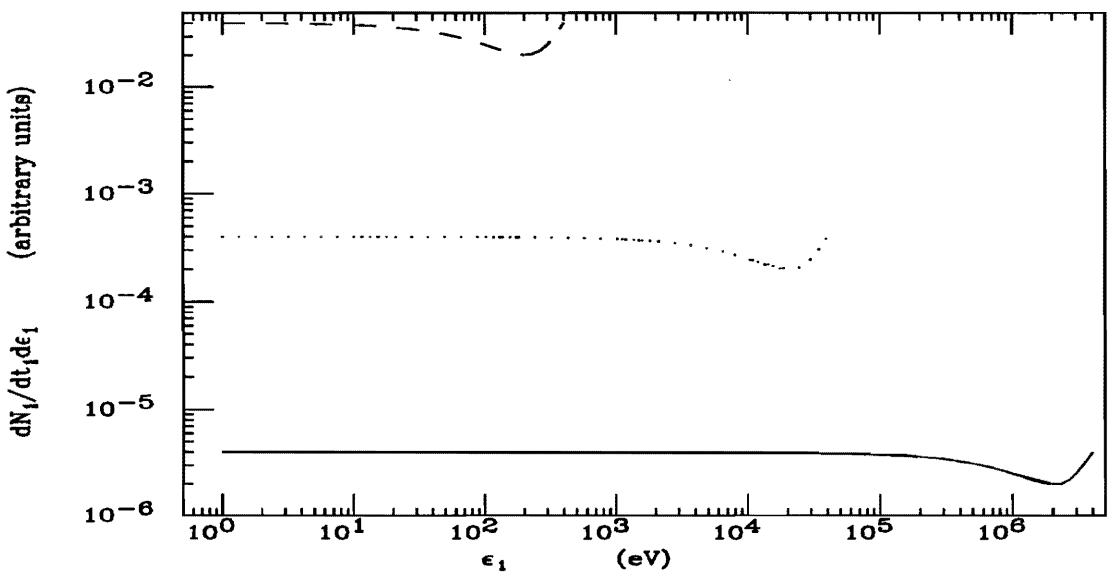
$dN_1/dt_1d\epsilon_1$ (arbitrary units)
10^{-2}
10^{-3}
10^{-4}
10^{-5}
10^{-6}
10^0
10^1
10^2
10^3
10^4
10^5
10^6
ϵ_1 (eV)

Figure 4:

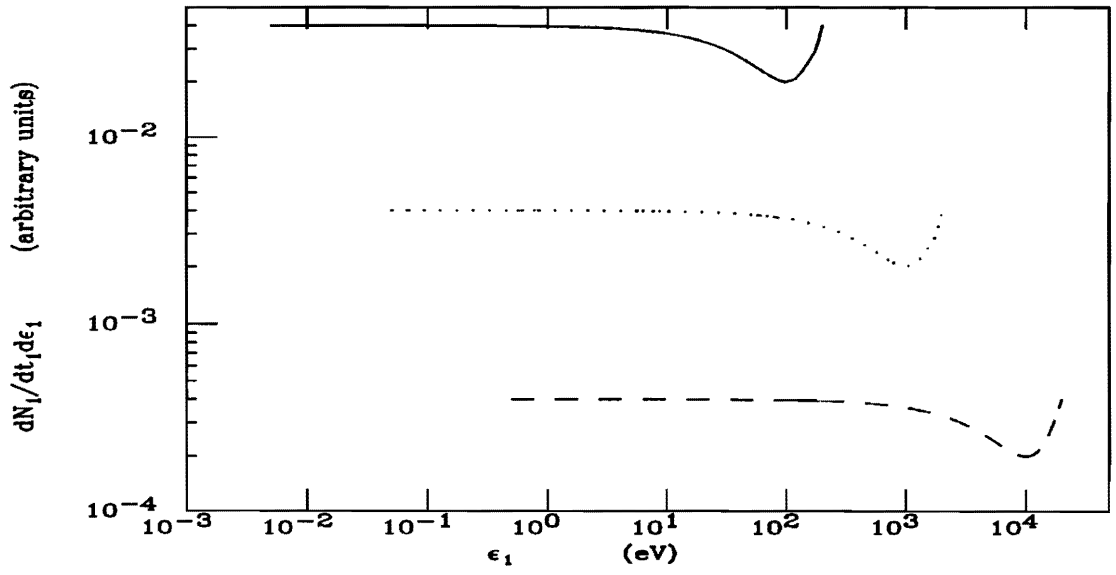
$dN_1/dt_1d\epsilon_1$ (arbitrary units)
10^{-2}
10^{-3}
10^{-4}
10^{-3}
10^{-2}
10^{-1}
10^{0}
10^{1}
10^{2}
10^{3}
10^{4}
ϵ_1 (eV)

Figure 5:

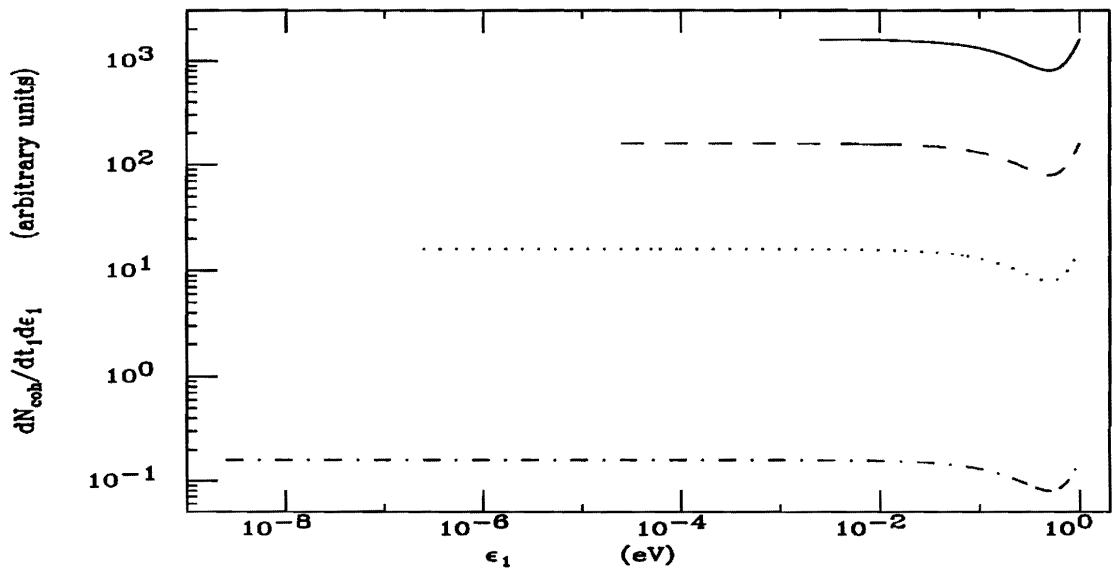
$dN_{cob}/dt_1d\epsilon_1$ (arbitrary units)
10^3
10^2
10^1
10^0
10^{-1}
10^{-8}
10^{-6}
10^{-4}
10^{-2}
10^0
ϵ_1 (eV)

Figure 6:

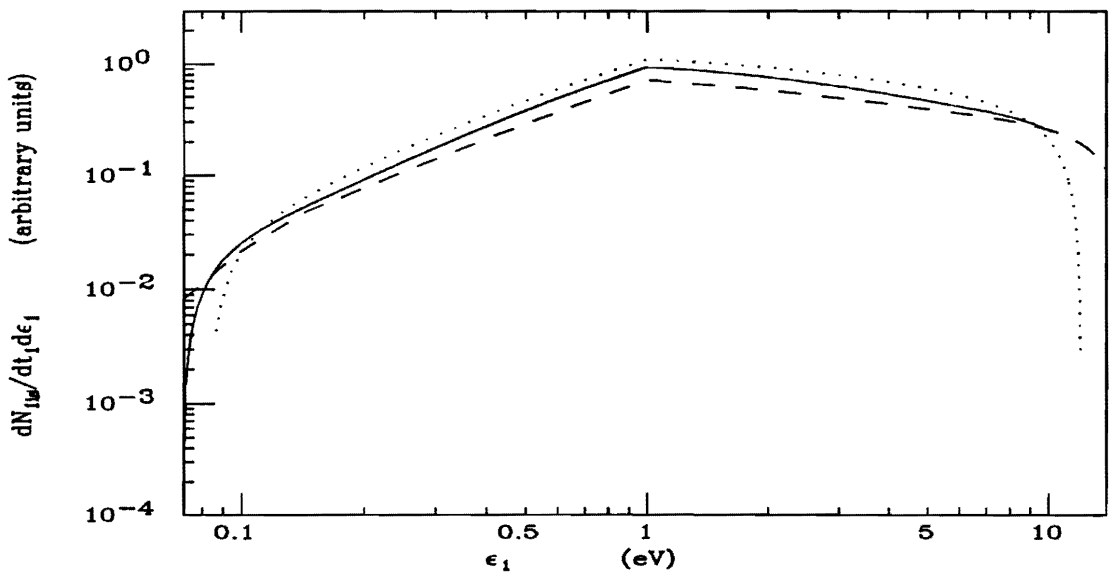
10^0
10^{-1}
10^{-2}
10^{-3}
10^{-4}
$dN_{1\nu}/dt_1 d\epsilon_1$ (arbitrary units)
0.1
0.5
1
5
10
ϵ_1 (eV)

Figure 7:

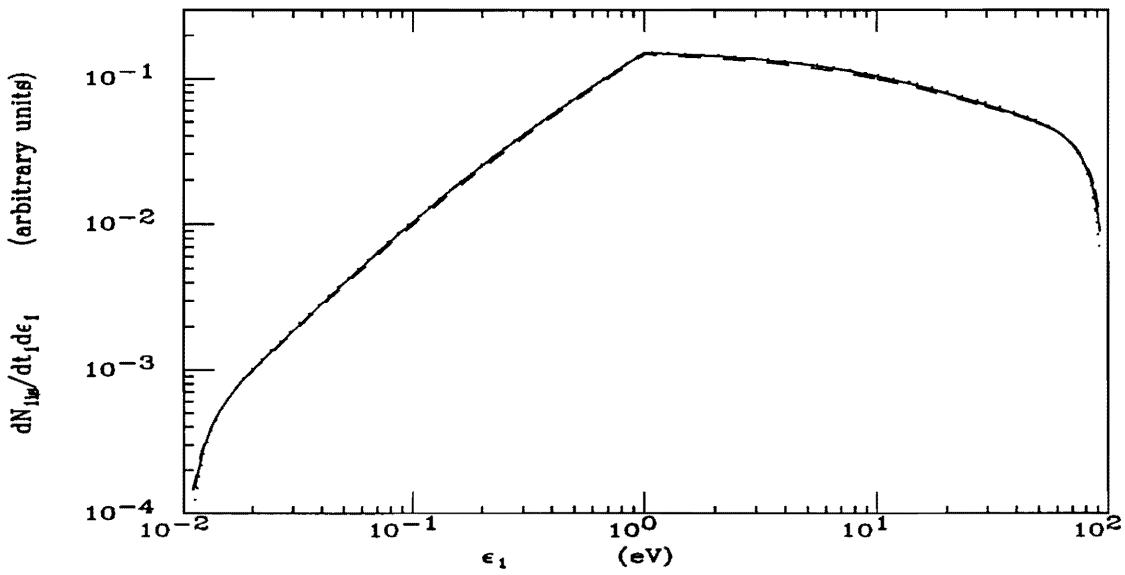
$dN_{i\mu}/dt_i d\epsilon_i$ (arbitrary units)
10^{-1}
10^{-2}
10^{-3}
10^{-4}
10^{-2}
10^{-1}
10^{0}
10^{1}
10^{2}
ϵ_i (eV)

Figure 8: